

DOI: 10.1002/sml.200500460

Tetrahedral Zinc Blende Tin Sulfide Nano- and Microcrystals**

Eric C. Greyson, Jeremy E. Barton, and Teri W. Odom*

This Communication describes a simple, seedless solution route to zinc blende (ZB) tin sulfide (SnS) nano- and microcrystals with tetrahedral morphology. These particles are unusual because 1) their shape is three-dimensional and highly symmetric, 2) their ZB crystal structure is different from the bulk orthorhombic structure, and 3) they exhibit optical properties distinct from orthorhombic particles at near-infrared (IR) wavelengths. Control over the crystal structure of a material is important for uncovering new phenomena since the local coordination can dramatically influence physical properties.^[1] The synthesis of metal chalcogenide and metal oxide nanoparticles with controlled size and shape has typically been by solution methods;^[2–4] in most cases, the nanoparticles retained their bulk crystal structure. Systems such as CdSe^[5] and ZnSe,^[6] which crystallize in both ZB and wurtzite forms, can be forced to nucleate and grow preferentially in either phase depending on the temperature of the reaction and the concentrations of the precursors. A recent study has shown that the efficiency of nanocrystal doping depends strongly on the crystal structure of the growing particle and the available faces for binding.^[7]

SnS is an important optoelectronic material that is usually found in the orthorhombic crystal structure.^[8] This semiconductor has received much attention for solar cell and photoconductor applications because it is inexpensive and nontoxic, is stable under ambient conditions, and has high conductivity (hole mobility = 90 cm² V⁻¹ s⁻¹) and absorption coefficients ($\approx 10^4$ cm⁻¹ near the fundamental absorption edge).^[8] The optical properties of SnS vary depending on the synthetic or fabrication method, but most work agrees on a direct bandgap at 1.296 eV and an indirect bandgap at 1.095 eV.^[8] Although films of SnS have been prepared and

studied extensively, there are few reports on the synthesis of well-formed SnS particles, which could potentially exhibit properties different from the bulk material. The ability to tune the optical properties of SnS could enable interesting optoelectronic applications. Solvothermal methods, using a combination of tin chloride and thiourea or elemental Sn and S, have produced 0D spherical particles or 1D whiskers with an orthorhombic structure.^[9–11] Herein we report the growth of 3D tetrahedral crystals of SnS with the ZB structure. We achieved a morphological yield greater than 90%, and by increasing the reaction temperature, produced 2D plates of SnS with an orthorhombic structure.

Nano- and microcrystals of SnS were formed by thermally decomposing tin chloride (SnCl₂) and elemental sulfur in a primary amine solvent. Oleylamine (10 mL) was heated to 170 °C in one flask, while anhydrous SnCl₂ (1.1 mmol) and S (1 mmol) were dissolved in a separate flask containing 5 mL of warm (60 °C) oleylamine. This warm mixture was injected by syringe into the hot (170 °C) amine under rapid stirring. The orange solution gradually grew darker after two hours of reaction, and then quickly turned a cloudy black color. The solid, black product was isolated from the amine, and excess precursors were removed by centrifugation in ethanol.

Scanning electron micrograph (SEM) images revealed that the SnS particles were tetrahedral in shape (Figure 1a). The majority of the tetrahedra were 200–300 nm on a side, while other tetrahedra had sides as small as 20 nm. The crystals synthesized by this preparation were always polydisperse in size, but the average particle size could be controlled by modifying the reaction time. Tetrahedra with edge lengths of several micrometers were observed after a reaction time of 12 h (Figure 1a, inset), although there were still small (<100 nm) tetrahedra present. No difference in size or shape of the SnS crystals was observed upon changing the amine surfactant (decyl-, dodecyl-, hexadecyl-, and oleylamine) while keeping the other reaction conditions the same.

Surprisingly, the crystal structure of the tetrahedra, determined by powder X-ray diffraction (PXRD), did not match orthorhombic SnS, but was consistent with a ZB structure with lattice constants $a = b = c = 5.845$ Å (Figure 1c and d). The assignment of the ZB phase for the nanocrystals is notable because bulk SnS had only been reported in the ZB phase by epitaxial growth on a NaCl seed layer.^[12,13] The PXRD also showed some small additional peaks from trace impurities (most likely Sn, S, Sn(OH)₂, and orthorhombic SnS). The appearance of the tetrahedral particles can be visualized by considering a ZB crystal terminated by half of its eight (111) faces. Because the (111) faces of a ZB crystal are inherently polar (see Supporting Information), the faces have different surface free energies, which can affect how the surfactant binds. Four non-adjacent (111) faces are equivalent and are terminated either with a Sn atom with a single dangling bond or an S atom with three dangling bonds, while the other four (111) faces are terminated by a Sn atom with three dangling bonds or an S atom with one dangling bond. The polarity of the (111) faces in similar materials systems with ZB structures has resulted in

[*] E. C. Greyson, J. E. Barton, Prof. T. W. Odom
Department of Chemistry, Northwestern University
2145 Sheridan Road, Evanston, IL 60208 (USA)
Fax: (+1) 847-491-7713
E-mail: todom@northwestern.edu

[**] This research was supported by an NSF CAREER Award (CHE-0349302). This work made use of the NUANCE Center facilities, which are supported by NSF-MRSEC, NSF-NSEC, Keck Foundation and Northwestern University. We thank Prof. Art Freeman and S.H. Rhim for performing electronic band structure calculations on the ZB SnS crystal structure. T.W.O. is an Alfred P. Sloan Research Fellow, a Cottrell Scholar of Research Corporation, a DuPont Young Professor, and a David and Lucile Packard Fellow.

Supporting information for this article is available on the WWW under <http://www.small-journal.com> or from the author.

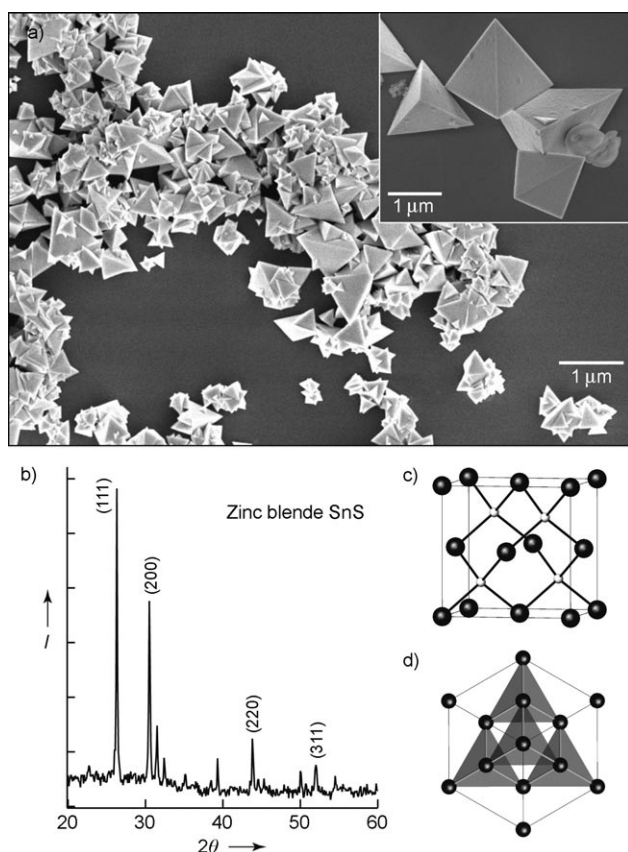


Figure 1. a) SEM image of zinc blende (ZB) tetrahedra of SnS after a reaction time of 3 h (inset: micrometer-sized tetrahedra synthesized after a reaction time of 12 h). The structures have sharp tips and edges with very smooth faces. b) PXRD confirming the structure of the tetrahedra as ZB. c) Cubic unit cell of ZB SnS viewed off the (100) axis. Sn^{2+} ions are indicated by (○) and S^{2-} ions are denoted by (●). d) ZB crystal viewed down the (111) axis.

the formation of CdS and CdTe tetrapods, which have wurtzite arms growing from a ZB core.^[14–16]

Selected-area electron diffraction (SAED) was used to confirm whether the tetrahedra were single-crystalline. When the C_3 rotational axis of a tetrahedron was parallel to the electron beam, the diffraction pattern showed the expected sixfold symmetry (Figure 2a). High-resolution transmission electron microscopy (HRTEM) revealed a lattice spacing of $8.1 \pm 0.2 \text{ \AA}$ for (110) fringes running from one vertex to the base of the opposite edge (Figure 2c and d). This spacing agrees (within 1.7%) with the lattice constant ($a = 5.845 \text{ \AA}$) determined from PXRD.

The ZB tetrahedra were formed under relatively mild temperatures (170°C), which might explain why this structure and morphology were not observed earlier by solution methods, since typical reaction temperatures exceed 250°C . To determine whether the particles were stable at elevated temperatures, we heated the tetrahedra under dry and wet conditions. We annealed SnS tetrahedra in a 1 in. tube furnace under Ar at 300°C for 3 h but observed no change in either the morphology or crystal structure of the tetrahedra. In contrast, SnS tetrahedra heated to 250°C in oleylamine

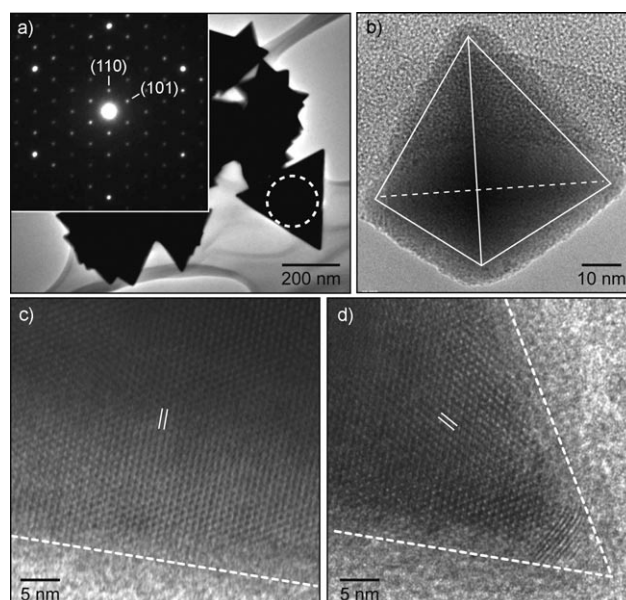


Figure 2. a) SAED of a single tetrahedron whose (111) axis is parallel to the electron beam. The expected sixfold symmetry is observed. The dashed circle indicates the area on the particle contributing to the diffraction. b) TEM image indicating the 3D structure of a tetrahedron. A model is overlaid to guide the eye. c) HRTEM image of an edge of a tetrahedron. The dashed white line indicates the edge of the tetrahedron, while the two small lines denote (110) fringes, which are perpendicular to the edge and spaced by 8.1 \AA . d) HRTEM image of (110) fringes bisecting a corner of the tetrahedron (dashed lines denote edges).

for 3 h underwent nearly complete ($>90\%$) conversion from ZB tetrahedra to orthorhombic plates (see Supporting Information). We hypothesize that the tetrahedra could convert in solution and not under Ar because the surfactant may lower the energy needed to change phases by stabilizing an intermediate.

Orthorhombic plates of SnS were grown without a tetrahedral intermediate when the reaction was performed at temperatures between 230 and 300°C . Early aliquots revealed very small ($<20 \text{ nm}$ on each side) plates (Figure 3a), while micrometer-sized, 2D plates were formed after 12 h (Figure 3a, inset). PXRD (PDF No. 73-1859) of the SnS plates matched the bulk orthorhombic crystal structure (Figure 3b). Based on PXRD spectra and TEM images, individual plates were typically oriented with their a axis perpendicular to the substrate. Although the edges of most small plates were terminated by (010) and (001) planes, Figure 4a shows that some large plates had edges that were terminated by (011) planes. Individual plates were also found to be single-crystalline with twofold symmetry (Figure 4b), and HRTEM images of an edge revealed lattice planes separated by 4.0 \AA , the spacing between (010) planes in orthorhombic SnS (Figure 4c). Figure 4d depicts the orthorhombic structure of SnS viewed down the (100) axis, which is quite different from the ZB structure of the tetrahedra.

We characterized the visible and near-infrared absorption of the SnS crystals using diffuse reflectance infrared Fourier transform spectroscopy (DRIFTS; Figure 5). The

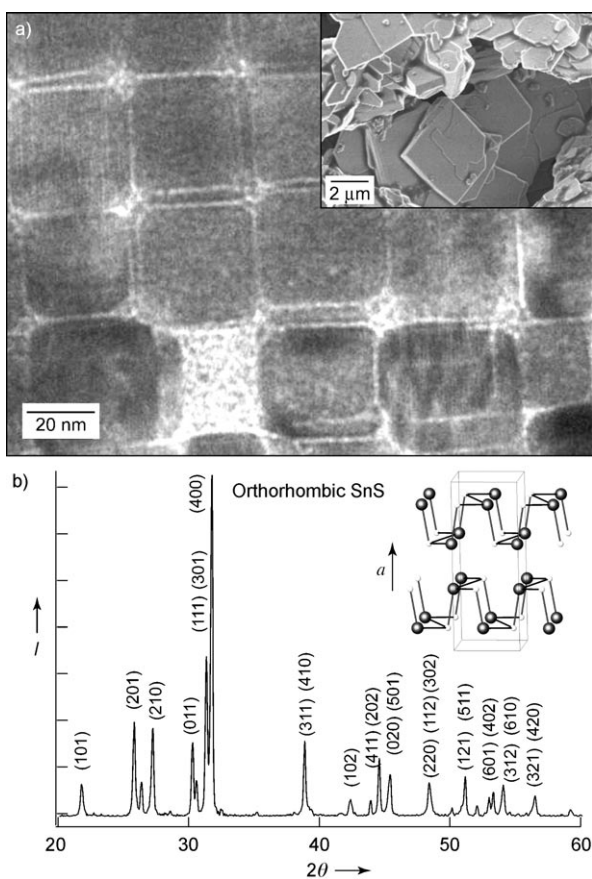


Figure 3. a) SEM images of 2D orthorhombic plates of SnS after a reaction time of 10 min. The plates are terminated by (010) and (001) or (011) edges (inset: micrometer-sized plates synthesized after a reaction time of 3 h). b) PXRD of the plates, which matches the orthorhombic structure (inset) of bulk SnS.

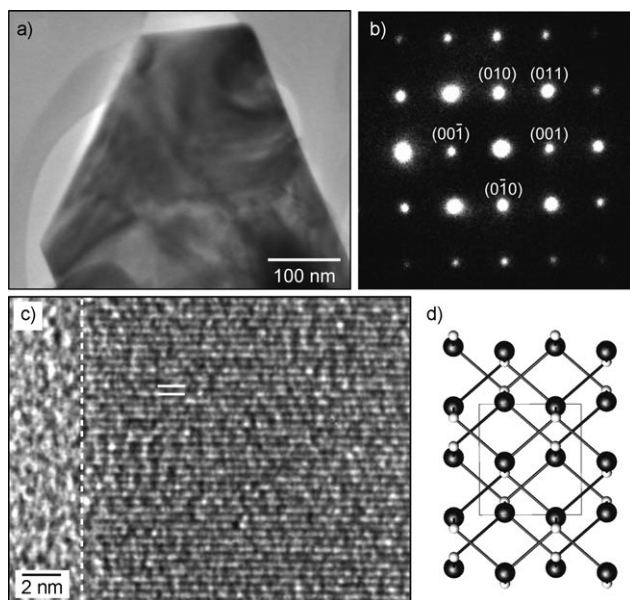


Figure 4. a) TEM image of a plate. b) SAED of the plate in (a) with the electron beam parallel to the (100) axis. c) HRTEM image of an edge of a 2D plate with (010) fringes perpendicular to the plate edge. The spacing is 4.0 Å. d) Orthorhombic SnS viewed down the (100) axis.

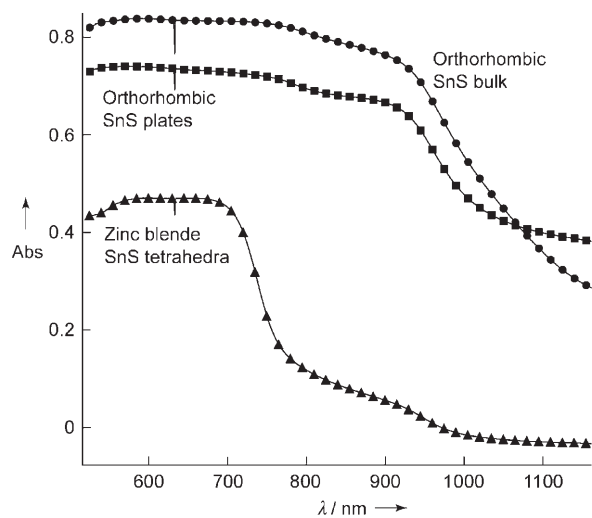


Figure 5. Absorption measurements of three samples of SnS: bulk, orthorhombic plates, and ZB tetrahedra. The orthorhombic plates (■) match the commercial bulk SnS (●) while ZB tetrahedra (▲) exhibit an absorption edge that is strongly blue-shifted.

absorption profiles of the orthorhombic SnS plates matched that of commercial bulk SnS (Alfa Aesar, 99.5%), exhibiting a strong absorption onset around 980 nm because of the direct bandgap, and a weaker absorption edge near 1100 nm from the indirect bandgap. The optical properties of the ZB tetrahedra were notably different, having a strong absorption edge around 700 nm, and only a gradual rise around 1000 nm. This absorption edge in the visible region could potentially enable ZB SnS to be used in photoconductor applications. The tetrahedra in these measurements were 200–300 nm on an edge, and hence the observed blue shift cannot be attributed to quantum confinement effects. It is well-known that the band structure depends critically on the types of orbital interactions in a solid and the symmetry of their overlap.^[1] Preliminary calculations using screened-exchange local density approximation density functional theory (sX-LDA DFT) predict ZB SnS to be either a metal or a small-indirect-bandgap semiconductor based on the lattice parameters. Thus, the observed optical behavior of the tetrahedral particles (which exhibit a smaller bandgap than the orthorhombic plates) emphasizes the importance of the crystal structure on the properties of SnS.

This Communication has presented a new, tetrahedral morphology of SnS that crystallizes in the ZB structure. These nano- and microcrystals were grown by a seedless solution route with a morphological yield greater than 90%. The different local coordination of the atoms in the ZB phase relative to the orthorhombic phase resulted in strikingly different optical properties in the near-IR region. The formation of nanoparticles with crystal structures different from their bulk is important not only because it may aid in the facile doping of nanocrystals, but also because it provides another strategy to obtain unique optical properties without confinement effects.

Experimental Section

SnS particles were prepared from a mixture of SnCl₂ (Aldrich, 99.99+%), and elemental S (Strem, 99+%) in oleylamine using Schlenk techniques. SnCl₂ and S were used as purchased, while oleylamine was distilled and degassed (>10 min) before use. Oleylamine (10 mL) was heated to the reaction temperature (170 °C for tetrahedra, ≥ 230 °C for plates) in a round-bottomed flask, while SnCl₂ (1.1 mmol) and elemental S (1 mmol) were dissolved in warm (60 °C) oleylamine (5 mL) in another flask for one hour. Once the precursors were completely dissolved in the warm oleylamine, they were injected by syringe into the hot (170 or 230 °C) oleylamine. The clear orange solution became cloudy black in 3 h at 170 °C, or within a minute at 230 °C. After 3 h, the heating mantle was removed, and the flask was cooled to room temperature under N₂. The particles were cleaned by sonication in anhydrous ethanol for 5 min followed by centrifugation. The purification procedure was performed three times.

The synthetic conditions were modified by changing the ratio of the Sn and S precursors and using solvents other than amines. Dilute quantities of NaCl were also added to confirm that the reaction proceeded without a seed particle. Finally, attempts at generalizing this reaction for other metals starting from CdCl₂, ZnCl₂, and PbCl₂ were made. Details of these experiments can be found in the Supporting Information.

A Gemini Leo 1525 FE-SEM was used for SEM imaging at 3 keV. A Hitachi HF-2000 and H-8100 were used for TEM imaging, SAED and EDX, at 200 keV. PXRD was carried out using a Rigaku DMAX A with a 0.05° step size and 2 s collection time (CuKα with a Ni filter). Infrared absorption measurements were performed using DRIFTS (diffuse reflectance infrared Fourier transform spectroscopy) on a Thermo Nexus 870 FTIR with 8 cm⁻¹ resolution and 128 scans. NIR measurements used an InGaAs detector and an IR light source, while visible absorption measurements used a Si detector and a white (halogen bulb) light source.

Keywords:

chalcogenides • inorganic chemistry • nanocrystals • synthesis design • tin

- [1] R. Hoffman, *Angew. Chem.* **1987**, *99*, 871; *Angew. Chem. Int. Ed. Engl.* **1987**, *26*, 846.
- [2] T. Hyeon, *Chem. Commun.* **2003**, *8*, 927.
- [3] C. B. Murray, S. Sun, W. Gaschler, H. Doyle, T. A. Betley, C. R. Kagan, *IBM J. Res. Dev.* **2001**, *45*, 47.
- [4] T. Trindade, P. O'Brien, N. L. Pickett, *Chem. Mater.* **2001**, *13*, 3843.
- [5] L. Qu, X. Peng, *J. Am. Chem. Soc.* **2002**, *124*, 2049.
- [6] P. D. Cozzoli, L. Manna, M. L. Curri, S. Kudera, C. Giannini, M. Striccoli, A. Agostiano, *Chem. Mater.* **2005**, *17*, 1296.
- [7] S. C. Erwin, Z. Lu, M. I. Haftel, A. L. Efros, T. A. Kennedy, D. J. Norris, *Nature* **2005**, *436*, 91.
- [8] J. B. Johnson, H. Jones, B. S. Latham, J. D. Parker, R. D. Engelken, C. Barber, *Semicond. Sci. Technol.* **1999**, *14*, 501.
- [9] Y. Zhao, Z. Zhang, H. Dang, W. Liu, *Mater. Sci. Eng. B* **2004**, *113*, 175.
- [10] C. An, K. Tang, Y. Jin, Q. Liu, X. Chen, Y. Qian, *J. Cryst. Growth* **2003**, *252*, 581.
- [11] D. Chen, G. Z. Shen, K. B. Tang, S. J. Lei, H. G. Zheng, Y. T. Qian, *J. Cryst. Growth* **2004**, *260*, 469.
- [12] S. B. Badachhane, A. Goswami, *J. Phys. Soc. Jpn.* **1962**, *17*, 251.
- [13] A. N. Mariano, K. L. Chopra, *Appl. Phys. Lett.* **1967**, *10*, 282.
- [14] L. Manna, E. C. Scher, A. P. Alivisatos, *J. Am. Chem. Soc.* **2000**, *122*, 12700.
- [15] L. Manna, D. J. Milliron, A. Meisel, E. C. Scher, A. P. Alivisatos, *Nat. Mater.* **2003**, *2*, 382.
- [16] M. Chen, Y. Xie, J. Lu, Y. Xiong, S. Zhang, Y. Qian, X. Liu, *J. Mater. Chem.* **2002**, *12*, 748.

Received: November 22, 2005

Published online on December 28, 2005